Low-temperature behavior of spontaneous polarization in $LiNbO_3$ and $LiTaO_3$

A. M. Glass and M. E. Lines
Bell Laboratories, Murray Hill, New Jersey 07974
(Received 26 June 1975)

The low-temperature behavior of spontaneous polarization in $LiNbO_3$ and $LiTaO_3$ has been measured by direct charge integration techniques and by the dynamic pyroelectric method, which observes current response to absorbed radiation. Measurements are reported from above room temperature down to 5°K and the results of the two methods are compared. A theoretical derivation of the expected low-temperature contributions to spontaneous polarization from the soft mode and from other lattice modes, including acoustic modes, is given using the self-consistent phonon formalism. We find that the derived theoretical form $dP_s/dT = K_1 T^3 + K_2 T^{-1/2} e^{-\hbar\Omega/kT} + \cdots$, with K_1 and K_2 independent of temperature T can account quantitatively for observations up to $T \sim 30$–40°K. The term $K_1 T^3$ results from acoustic-mode population via strain and is positive in $LiNbO_3$ producing an initial increase in P_s with T at very low temperature. The exponential term arises from thermal population of a low-energy optic mode, not necessarily at long wavelengths, with a minimum energy gap $\hbar\Omega$, of order 60–70 cm^{-1} in both materials. This mode gives rise to a pronounced maximum in the dynamic response, which is observed experimentally near 30°K in both materials.

I. INTRODUCTION

The operation of pyroelectric materials as thermal detectors of infrared radiation is based on the change of spontaneous polarization $\delta P_s'$ of a pyroelectric crystal when it is heated by incident radiation through a temperature δT:

$$-\delta P_s'(\omega) = p\,\delta T(\omega)\,, \tag{1.1}$$

where p is the pyroelectric coefficient. The prime is included since we shall later show that P_s' is not exactly equal to P_s, the electric moment per unit volume, in a free crystal, although the difference $P_s' - P_s$ is relatively insignificant at all except the very lowest temperatures. For an incident power $I(\omega)$, sinusoidally modulated at frequency ω, the displacement current density $J(\omega)$ in the crystal is given by

$$\frac{J(\omega)}{I(\omega)} = \frac{ep}{C(1+1/\omega^2\tau^2)}\,, \tag{1.2}$$

where e is the fraction of incident light which thermalizes in the crystal, C is the thermal capacity, and τ is the thermal relaxation time of the crystal with its surroundings.

The performance of most detectors improves as the temperature is decreased because of the decrease in thermal noise. With pyroelectrics, though, p usually decreases with decreasing temperature, thereby decreasing the responsivity of (1.2), resulting in little, if any, improvement in detector performance. However, at sufficiently low temperatures the thermal capacity C decreases rapidly, which would tend to increase the responsivity, and the behavior of the ratio p/C at low temperature is not immediately obvious.

Early observations[1] of several pyroelectrics suggested that polarization deviation is proportional to T^2 at low temperatures, which implies that if the specific heat c_v follows a T^3 law according to Debye theory, then p/C would diverge at low temperatures—a result of great practical importance. These observations were accounted for by Born[2] within the Debye approximation assuming them to be second-order acoustic-mode contributions to constant strain polarization. Later data on ZnO,[3] however, showed that with reasonable accuracy p/C is constant between 10 and 40 °K. Using a model of a single anharmonic optic mode Garrett[4] could account for this behavior, but such a model is not applicable at low temperatures where the acoustic branches play a dominant role. The pyroelectric coefficient of lithium sulphate monohydrate, on the other hand, shows a change of sign at about 110 °K.[5,6] To account for this behavior, Lang[6] extended the Born theory by adding contributions from nondispersive optic modes to the pyroelectric effect. Agreement between theory and experiment was obtained with five independent oscillators, in addition to the acoustic modes, by adjusting the coefficients and frequencies to fit the pyroelectric and specific-heat data.

In this work we study directly the temperature dependence of the polarization and of the ratio p/C for $LiTaO_3$ and $LiNbO_3$, and account for the behavior in terms of the acoustic- and optic-mode spectra of these crystals, including the effects of dispersion in the Brillouin zone. These materials are isomorphous rhombohedral ferroelectrics belonging to the space group $R3c$ below the Curie temperature T_c ($T_c = 618$ °C for the $LiNbO_3$ crystal and $T_c \sim 1130$–1145 °C for the $LiNbO_3$ crystals used in this work). Below T_c, 22 infrared-active lattice modes ($4A_1 + 9E$) are expected. In the temperature range up to ~40 °K a single low-frequency optic mode is found to dominate the temperature dependence of the ratio p/C. Indeed direct measurement of the

ratio p/C provides a much more sensitive indicator of optic-mode contributions to the polarization than measurement of P_s' alone.

II. EXPERIMENTAL

A. Measurement of polarization change

The change of spontaneous polarization as a function of temperature was obtained by integrating the charge which appears on the polar faces of the crystal with an operational amplifier.[7] With this arrangement the field across the crystal is essentially zero at all times, and the polarization change can be recorded continuously as a function of temperature.

Several crystals of typical dimensions 0.7 cm on a side were electroded with gold on the faces normal to the polar axis. The crystals were mounted in an unclamped manner in a helium gas flow Dewar[7] so that the temperature could be varied continuously from 5 to 400 °K.

Typical results are shown in Figs. 1(a) and 1(b) for $LiTaO_3$ and $LiNbO_3$. The smallest charge which could be measured with this setup was about 10^{-11} C over a 100-sec interval, so that fractional changes

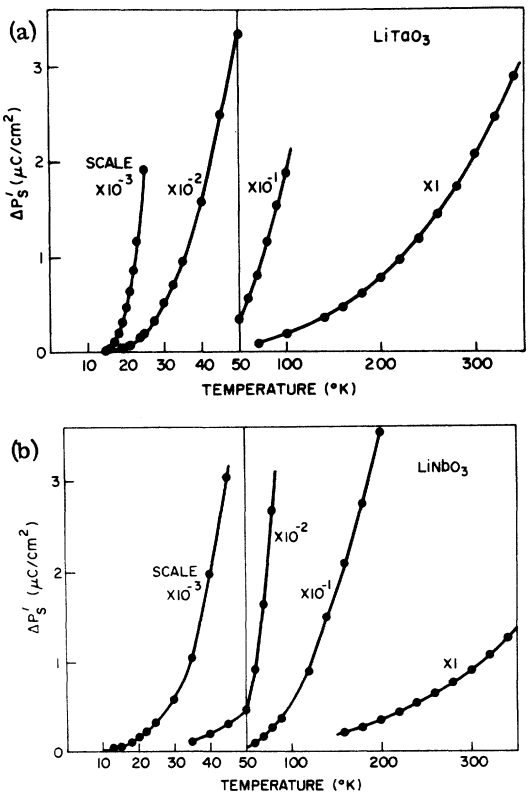

FIG. 1. (a) Change of spontaneous polarization with temperature for $LiTaO_3$ as measured by the charge integration technique of Sec. II A. Note the change of scale at 50 °K on the temperature axis. (b) As for (a) but for $LiNbO_3$.

of P_s' of about one part in 10^7 could be measured. All measurements were made at constant stress. Of course p can be obtained by differentiation of Figs. 1(a) and 1(b).

B. Measurement of p/C

The ratio of the pyroelectric coefficient to thermal capacity was measured directly from the current response of the crystals to the absorbed radiation, according to Eq. (1.2), using the dynamic technique of Chynoweth.[8] The crystals were mounted as before in a gas flow Dewar with windows through which the crystal could be illuminated by a filtered tungsten lamp (wavelength range 0.6–4 μm).

The modulation frequency (1 kHz) of the incident light was well below any piezoelectric resonance frequencies of the crystal to avoid inertial clamping. The light was chopped with a duty cycle of 1 : 4 to minimize heating of the crystal at low temperatures. The 200-μsec "on" time was shorter than the thermal relaxation time of the crystal with the surroundings ($\omega\tau \ll 1$) at all temperatures. This was checked by observation of the waveform of the current response. The time constant of the measuring circuit was much less than 200 μsec.

With this technique it is difficult to ensure that the crystal is uniformly heated. Two experimental geometries were used: In one the radiation was absorbed directly at the front electrode, and the crystal was heated by thermal diffusion from the surface; and in the second arrangement edge electrodes were used (polar axis normal to the incident radiation), and the light was absorbed in the crystal volume. Even with this geometry there was significant absorption at the electrodes. Furthermore the crystal surface is in intimate contact with the helium gas, giving rise to further temperature gradients in the bulk. Both experimental geometries gave the same temperature dependence of the pyroelectric response, but clamping effects due to inhomogeneous heating cannot be ruled out. Indeed the theoretical analysis suggests that clamping effects are significant.

With this dynamic technique only relative measurements of p/C are accurate. Absolute calibration can be made at room temperature using the pyroelectric data of Figs. 1(a) and 1(b) and values of C of ~22 and ~24 cal mole^{-1} °C^{-1} for $LiNbO_3$ and $LiTaO_3$, respectively.[9,10]

Typical results are shown in Figs. 2(a) and 2(b). A peak in the pyroelectric response is observed around 30 °K in both $LiTaO_3$ and $LiNbO_3$ followed by a sharp drop below this temperature. Pyroelectric response was still easily observable down to 5 °K. It is clear from Figs. 1 and 2 that direct measurement of the ratio p/C gives greatly increased sensitivity at low temperatures than would be obtained

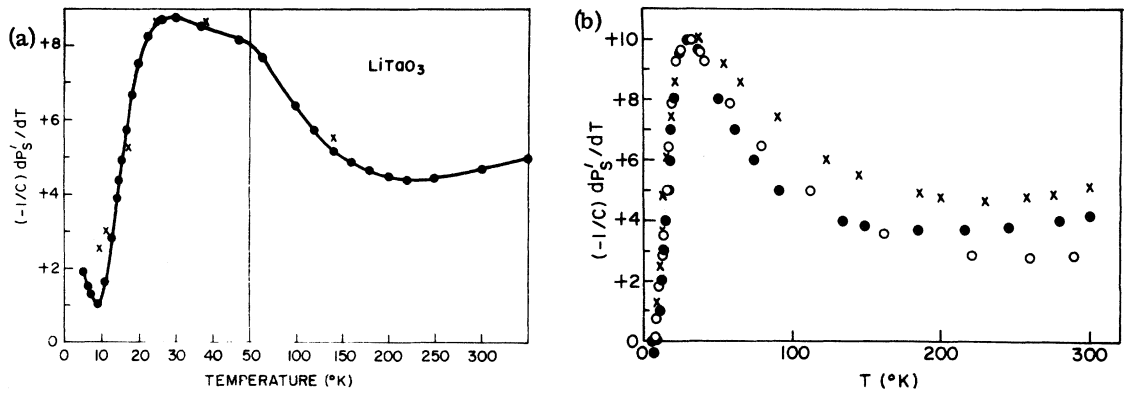

FIG. 2. (a) Ratio of pyroelectric coefficient $p=-dP_s'/dT$ to thermal capacity C as measured for $LiTaO_3$ by the infrared detection technique of Sec. II B. Only relative measurements are accurate, although an approximate calibration of the ordinate can be made from the room-temperature values $dP_s'/dT \approx -18\times10^{-3}$ $\mu C/cm^2\,°K$ [from Fig. 1(a)] and $C \approx 24$ cal/mole °K. Also shown (crosses) are equivalent measurements for an effectively clamped crystal (see text). (b) Ratio of pyroelectric coefficient $p=-dP_s'/dT$ to thermal capacity C as measured for three different samples of $LiNbO_3$ by the infrared detection technique of Sec. III B. Open circles denote measurements made on a $^6LiNbO_3$ sample with a stoichiometric Li : Nb composition ratio in the melt of 50 : 50; closed circles on a 50 : 50 sample of $^7LiNbO_3$, and crosses on a Li-deficient (congruent melt) 48.6 : 51.4 sample of $^7LiNbO_3$. Measurements have been arbitrarily normalized at the low-temperature peak value of response. An approximate calibration can be obtained only for the Li-deficient sample (crosses), which was the sample used for the charge integration measurements of Fig. 1(b), by noting the approximate room-temperature values $dP_s'/dT \approx -8.3\times10^{-3}$ $\mu C/cm^2\,°K$ [from Fig. 1(b)] and $C \approx 22$ cal/mole °K.

from independent measurement of p and C.

The main experimental error was the measurement of temperature itself. A carbon resistance thermometer close to the crystal, but not in contact, was used to measure the temperature below 100 °K, and in a gas flow Dewar some error may be expected at low temperatures. Moving the thermometer did not vary the temperature by more than 2 °K at 30 °K and $\frac{1}{2}$ °K at 5 °K.

The pyroelectric response of the unclamped crystals includes both the primary pyroelectric response and the secondary pyroelectric response due to thermal expansion and the piezoelectric effect. To determine whether any of the main features of Fig. 2 were due to piezoelectric effects, inertially clamped measurements of p/C were also made. Instead of the tungsten lamp and chopper, a pulsed rhodamine 6-G dye laser at 6000 Å was used with a pulse duration of 150 nsec and an energy of about 1 mJ. The crystal was effectively clamped since the fundamental resonances were at frequencies below 1 MHz. The integrated current response $\delta P_s' = \int_0^\infty J\,dt$ of the crystal to a single pulse is shown in Fig. 3. The initial fast pyroelectric response is followed by piezoelectric resonances. The initial response is plotted on Fig. 2(a) together with the low-frequency data. It is seen that the general features of the high- and low-frequency responses are the same, but there are some differences at the lowest temperatures. This may be due to the fact that at low temperatures the piezoelectric resonances became very large (and slowly decaying), making accurate measurement of the primary effect difficult. Furthermore, at low temperatures the crystal temperature may rise significantly during a single pulse leading to inaccuracy in the measurements of p/C.

III. THEORY: SOFT-MODE CONTRIBUTION TO POLARIZATION

In $LiNbO_3$ and $LiTaO_3$ the soft mode is an A_1-symmetry long-wavelength ($\vec{q}\to 0$) transverse-optic phonon describing a mean ionic motion or displacement along the polar c axis. Its frequency rises with decreasing temperature from essentially zero at T_c to in excess of 200 cm^{-1} as $T\to 0$ °K.[11,12] In both the tantalate and niobate this soft mode is the lowest-frequency $\vec{q}=0$ polar c-axis mode throughout this temperature region, and also has a mode strength an order of magnitude larger than any other optic mode of like symmetry. It follows that

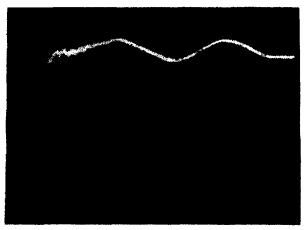

FIG. 3. Oscilloscope trace showing the initial clamped pyroelectric response $\Delta P'$ followed by slowly varying oscillations due to secondary pyroelectricity upon thermal expansion of the crystal.

a fairly good self-consistent description of the temperature development of the soft mode should be given by a single-mode approximation.

For example, let us describe the motion of ions in the lth primitive lattice cell, with the symmetry of the soft mode, by local mode conjugate displacement and momentum operators ξ_l and π_l. These could, of course, be formally related to the individual momenta and displacements of each constituent ion in the cell. In the single-mode approximation we now express the ion-displacement Hamiltonian for the macroscopic crystal as

$$\mathcal{H} = \frac{1}{2}\sum_l \pi_l^2 + \sum_l V(\xi_l^2) - \frac{1}{2}\sum_l \sum_{l'} v_{ll'}\xi_l \xi_{l'} , \quad (3.1)$$

where V is an anharmonic local potential function (describing the motion of an isolated primitive cell) and $v_{ll'}$ provides a representation of intercell interactions. The statistical description of (3.1) in terms of temperature-dependent phonons is readily obtained in the so-called self-consistent phonon approximation[13] as follows.

Using (3.1), the equation of motion for displacement can be written (both classically and quantum mechanically)

$$\ddot{\xi}_l = \sum_{l'} v_{ll'}\xi_{l'} - \frac{\partial V(\xi_l^2)}{\partial \xi_l} . \quad (3.2)$$

At a particular temperature T, let the mean displacement $\langle \xi_l \rangle$, which is cell independent, be denoted $\xi_0(T)$. Expressing ξ_l in terms of its deviation from the thermal average, we can rewrite (3.2) as a function of $u_l = \xi_l - \xi_0(T)$,

$$\ddot{u}_l = \sum_{l'} v_{ll'}[\xi_0(T) + u_{l'}] - \frac{\partial}{\partial u_l} V[\xi_0(T) + u_l]^2 . \quad (3.3)$$

Let us define the expansion

$$V(\xi_l^2) = \sum_{n=0}^{\infty} a_n \xi_l^{2n} . \quad (3.4)$$

Equation (3.3) becomes

$$\ddot{u}_l = \sum_{l'} v_{ll'}[\xi_0(T) + u_{l'}] - \sum_n 2n a_n [\xi_0(T) + u_l]^{2n-1} . \quad (3.5)$$

We now make the basic assumption of self-consistent phonon theory, namely, that the ensuing motion is quasiharmonic about $\xi_0(T)$. In other words $\langle \ddot{u}_l \rangle = \langle u_l \rangle = 0$. Expanding (3.5) as a series in powers of $u_l/\xi_0(T)$, assuming this parameter to be small (i.e., low temperatures), and taking thermal averages on both sides, we find

$$\sum_{l'} v_{ll'} = \sum_{n=1}^{\infty} 2n a_n \xi_0^{2n-2}(T)\{1 + (n-1)(2n-1)[\langle u_l^2 \rangle / \xi_0^2(T)]\} \quad (3.6)$$

to lowest order in $\langle u_l^2 \rangle / \xi_0^2(T)$. This equation expresses the temperature dependence of $\xi_0(T)$ (or, in other words, of soft-mode polarization) in terms of the mean-square displacement $\langle u_l^2 \rangle$. To evaluate the latter we subtract (3.6) from (3.5) and introduce running waves

$$u_{\vec{q}} = \left(\frac{1}{N}\right)^{1/2} \sum_l u_l e^{i\vec{q}\cdot\vec{l}} , \quad (3.7)$$

where $\vec{q}$ is a wave vector and N is the number of cells in the macroscopic lattice. Linearizing the resulting equation by thermally approximating $u_{\vec{q}} u_{\vec{q}'} u_{\vec{q}''}$ by $u_q \langle u_{q'} u_{q''} \rangle$ for all $\vec{q}'$ and $\vec{q}''$ we find a renormalized harmonic-oscillator form

$$\ddot{u}_{\vec{q}} = -\Omega_{\vec{q}}^2(T) u_{\vec{q}} , \quad (3.8)$$

where

$$v(\vec{q}) + \Omega_{\vec{q}}^2(T) = \sum_{n=1}^{\infty} 2n(2n-1) a_n \xi_0^{2n-2}(T) \times \{1 + (n-1)(2n-3)[\langle u_l^2 \rangle / \xi_0^2(T)]\} , \quad (3.9)$$

with

$$v(\vec{q}) = \sum_{l'} v_{ll'} e^{i\vec{q}\cdot(\vec{l}'-\vec{l})} , \quad (3.10)$$

again working to first order in $\langle u_l^2 \rangle / \xi_0^2(T)$. The standard statistical result for quantum oscillators

$$\langle u_l^2 \rangle = N^{-1} \sum_{\vec{q}} \frac{\hbar}{2\Omega_{\vec{q}}} \coth \frac{\hbar \Omega_{\vec{q}}}{2kT} \quad (3.11)$$

now completes the self-consistent phonon picture and closes the set of equations (3.6), (3.9), and (3.11) for the temperature dependence of soft-mode polarization and soft-mode frequency at low temperatures.

We now compare Eq. (3.6) at temperature T with the same equation at absolute zero. Defining a normalized polarization deviation $\epsilon = [\xi_0(0) - \xi_0(T)]/\xi_0(0)$ we obtain, to first order in ϵ,

$$\epsilon = \frac{1}{2}\left(\frac{\partial^3 V}{\partial \xi_l^3}\right)_0 \frac{\langle u_l^2 \rangle_T - \langle u_l^2 \rangle_0}{\xi_0(0)\Omega_0^2(0)} , \quad (3.12)$$

where the derivative is taken at $\xi = \xi_0(0)$ and where $\Omega_0(0)$ is the $T = 0$ zone-center soft-mode frequency. For cases where the dominant anharmonicity is of lowest possible order (e.g., fourth order, $n = 2$) this expression simplifies further to

$$\epsilon = \tfrac{3}{2}(\langle u_l^2 \rangle_T - \langle u_l^2 \rangle_0)/\xi_0^2(0) . \quad (3.13)$$

Using the latter expression for illustrative purposes [although as far as T dependence is concerned both (3.12) and (3.13) are identical] and approximating $\coth x$ by $1 + 2e^{-2x}$ for values of $x > 1$, we now combine (3.13) and (3.11) to find

$$\epsilon = 3[2\xi_0^2(0)]^{-1} \langle [\hbar/\Omega_{\vec{q}}(T)] e^{-\hbar\Omega_{\vec{q}}(T)/kT} \rangle_{\vec{q}} , \quad (3.14)$$

where $\langle \cdots \rangle_{\vec{q}}$ indicates an average over the first Brillouin zone of the reciprocal lattice.

For temperatures of interest in the present experiments (viz., below room temperature) Raman and infrared absorption experiments[11,12] indicate

that any temperature variation of the soft mode (or of any other optic mode, for that matter) is quite small in $LiTaO_3$ and $LiNbO_3$. We shall therefore neglect any mode softening and replace $\Omega_{\vec{q}}(T)$ by $\Omega_{\vec{q}}(0)$. In this approximation the full self-consistency of the earlier equations is not employed, and the subsequent findings would also result from a straightforward perturbational approach. We prefer the more general formalism since it is mathematically no more difficult and yet allows the mechanism of mode softening to be appreciated. To perform the Brillouin-zone average in (3.14) requires a knowledge of the frequency dependence of the soft mode. From inelastic neutron scattering data (Chowdhury *et al.*[14]) dispersion is fairly flat in the direction of the c axis for which measurements have been made. If we neglect any $\vec{q}$ dependence of the mode and write $\Omega_q(0) = \Omega_0$, Eq. (3.14) gives

$$\epsilon \propto e^{-1/t} , \tag{3.15}$$

in which $t = kT/\hbar\Omega_0$. By direct differentiation we find a soft-mode contribution to p of form

$$p \propto \frac{d\epsilon}{dT} = Kt^{-2} e^{-1/t} , \tag{3.16}$$

in which K is a temperature-independent parameter.

The effect of mode dispersion is to modify the t^{-2} factor in (3.16), but the exponential factor remains as a Boltzmann measure of the minimum energy gap associated with the band. At very low temperatures it may be a better approximation to assume a quadratic $\vec{q}$ dispersion close to the bottom of the band and write

$$\Omega_q(0) = \Omega_{\min}(0) + \alpha_x q_x^2 + \alpha_y q_y^2 + \alpha_z q_z^2 , \tag{3.17}$$

where α_x, α_y, α_z are constants. Substituting in (3.14) leads directly to the relationship

$$p \propto \frac{d\epsilon}{dT} = K' t^{-1/2} e^{-1/t} , \tag{3.18}$$

where K' is a constant and $t = kT/\hbar\Omega_{\min}(0)$. The presence of the exponential factor is to be contrasted with the analogous spin-wave situation in Heisenberg magnetism, for which the energy gap is absent, leading to a simple power-law temperature dependence for magnetization and its derivatives.

IV. INDIRECT CONTRIBUTIONS, THERMAL EXPANSION, PIEZOELECTRICITY

In addition to the direct contribution to the temperature dependence of spontaneous polarization discussed above there are a number of indirect effects which must be recognized. These can assume a great importance at low temperatures since the energy gap in the soft-mode dispersion, if the long-wavelength values are any guide, is likely to be quite large and give rise to a rapid exponential decay of soft-mode contributions in the low-temperature limit. Any indirect contribution involving a lattice mode of lower frequency must dominate the direct contribution to the temperature dependence of spontaneous polarization at sufficiently low temperatures.

Easiest to populate thermally are the transverse-acoustic modes of long wavelength. With no energy gap they can produce, via the mechanism of thermal expansion and the piezoelectric effect, a contribution which is not exponentially small at low temperatures. [They can even contribute to damped pyroelectric coefficient in second order,[2] but the latter so-called "Born" contribution to p/C diverges as $T \to 0$ and from Fig. 2 can be seen to be negligible in all samples at least above 10 °K. We shall therefore not consider it further in the present paper although the possibility that the lowest few data points in the sample of Fig. 2(a) may be due to this effect cannot be excluded completely.] In addition, there are other optic modes (the lower-energy E-symmetry phonons) which have a lower excitation energy than the $q \approx 0$ soft A_1 mode at low temperatures. The lowest zone-center E modes, as measured by Raman techniques, were initially claimed to be at 70 cm^{-1} ($LiTaO_3$) and 90 cm^{-1} ($LiNbO_3$) (Ref. 12), but more recent work[15,16] casts doubt on the earlier line assignment and suggests that the lowest $q = 0$ fundamental E modes may be ≈ 140 cm^{-1} ($LiTaO_3$) and ≈ 150 cm^{-1} ($LiNbO_3$), although some doubt remains. Such optic E modes will couple, in general, to strain and, via the piezoelectric effect, to polarization. Indeed there is evidence[12] that grown-in imperfections allow for a direct coupling of long-wavelength A_1 and E modes in present crystal specimens, so that a thermal population of $q \approx 0$ E modes can affect polarization in a direct dynamic fashion as well. We should also recognize the fact that, while these lower-frequency optic modes transform according to an E representation for all $\vec{q}$ within local mode theory (such as given in Sec. IV B), this is not true for finite values of $\vec{q}$ perpendicular to the polar c axis in a strict group-theoretical analysis of lattice dynamics in the $LiNbO_3$ structure.[17] Finally, since there are four optically active A_1 modes at low temperatures in both the tantalate and the niobate, they will all, in general, contribute to spontaneous polarization. However, since the most strongly polar A_1 mode is also the lowest in energy of these, we do not expect the others to contribute a significant amount in the temperature range of interest. This suggests that the acoustic and low-energy E-mode contributions are the most important secondary effects and we consider them in more detail below.

A. Thermal expansion

Consider a thin plate of ferroelectric $LiNbO_3$ or $LiTaO_3$ of plate area A and thickness L, with spontaneous polarization P_s normal to the plate, and at a temperature T. If condenser plates are attached to surfaces A, a charge Q develops on the plates just sufficient to balance the internal Maxwell field resulting from the spontaneous polarization, i.e.,

$$Q = P_s A \ . \tag{4.1}$$

If the temperature is now raised to $T+dT$, with a resulting thermal expansion $L \to L(1+\alpha_3 dT)$, $A \to A(1+2\alpha_1 dT)$, where α_1 and α_3 are linear thermal-expansion coefficients for the trigonally symmetric situation, the spontaneous polarization undergoes a shift dP_s (i.e., $P_s \to P_s + dP_s$) which is made up of two parts, the primary pyroelectric polarization dP_0 which would result if the crystal remained in a state of constant strain and a secondary polarization dP_1 induced by strain via the piezoelectric effect.[18] The former, dP_0, results from the soft-mode contribution plus any dynamic A_1-E mode coupling contribution. The latter, dP_1, can be expressed

$$dP_1 = d_{3i} c_{ij} \alpha_j \, dT \ , \tag{4.2}$$

where $i, j = 1, 2, 3$ label coordinate directions (with direction 3 parallel to the spontaneous polarization), repeated indices imply summation, d_{3i} are piezoelectric compliances, c_{ij} are elastic moduli, and α_j are the thermal-expansion coefficients. The material constants d_{3i} and c_{ij} are quite well documented for both $LiTaO_3$ and $LiNbO_3$.[19,20]

In the expanded situation at temperature $T+dT$, the condenser charge will adjust itself, $Q \to Q + dQ$, in such a way that it again cancels the total displacement charge, i.e.,

$$(Q+dQ)L(1+\alpha_3 dT) = (P_s + dP_s)LA(1+\alpha_3 dT + 2\alpha_1 dT) \ . \tag{4.3}$$

To first order the charge per unit area gained by the plates is

$$dP_s' = dQ/A = dP_s + 2\alpha_1 P_s dT$$
$$= dP_0 + d_{3i} c_{ij} \alpha_j dT + 2\alpha_1 P_s dT \ . \tag{4.4}$$

It is now clear that if the spontaneous polarization P_s is defined in the conventional fashion, namely, as electric dipole per unit volume, then the P_s' of Secs. I and II is not this same quantity. It is for this reason the prime was included in the earlier symbolism.

On the other hand the total electric moment $M = P_s AL$ of the sample increases by

$$dM = LA(dP_s + P_s \alpha_3 dT + 2P_s \alpha_1 dT) \tag{4.5}$$

or

$$dM/LA = dP_s' + P_s \alpha_3 dT \ . \tag{4.6}$$

Since L and A are by definition temperature-independent quantities, dM/LA describes a suitably normalized temperature dependence of total electric moment, i.e., an electric moment per unit mass.

It is clear therefore that our experiments measure a quantity $dQ/A = dP_s'$ which is different from electric moment per unit volume or per unit mass for a free crystal, although the difference between these quantities only becomes important at very low temperatures, as we shall see. This increment dP_s' is therefore given by Eq. (4.4) and contains two separate contributions originating from thermal expansion, one piezoelectric and the other not. We expect acoustic modes to contribute to both these expansion terms but, to the extent that there is significant optic-mode–to–strain coupling, we also anticipate contributions from both E and A_1 optic modes at temperatures for which they can be thermally populated to any significant degree.

B. Dynamic E-mode contributions

There is direct evidence from Raman scattering[12] that, even at long wavelengths for which the A_1 and E symmetry characterization is rigorous, there is a coupling between E and A_1 modes in both $LiTaO_3$ and $LiNbO_3$. Whatever the detailed origin of the effect (e.g., a presence of grown-in imperfections), the result is that the E modes now carry with them a certain small measure of c-axis polarization. We may analyze the temperature dependence of this contribution within local mode theory.

Representing the lth-cell E mode by its conjugate momentum and displacement coordinates π_l', ξ_l', we write the corresponding E-mode Hamiltonian for the macroscopic lattice [compare Eq. (3.1)], including a simple linear coupling to the soft-mode coordinate ξ, as

$$\mathcal{H}_E = \sum_l [\tfrac{1}{2}\pi_l'^2 + V_E(\xi_l'^2) - C'\xi_l'\xi_l] - \frac{1}{2}\sum_l \sum_{l'} v_{ll'}^{(E)} \xi_l' \xi_{l'}' \ , \tag{4.7}$$

where C' is an unspecified coupling constant. Since the motion of the soft mode is (at our temperatures of interest) closely centered about the equilibrium value $\xi_l = \xi_0(T)$, we shall approximate ξ_l in (4.7) by its average $\xi_0(T)$. The coupling term then becomes a simple effective field, and the analysis of Sec. III for Hamiltonian (3.1) can be followed with only minor changes.

Defining a deviation $u_l^{(E)}$ of ξ_l' from its mean value $\xi_0'(T)$, we again use the self-consistent phonon approximation. The new (effective field) terms enter explicitly only the equation for static displacement, which becomes

$$\left(2a_1^{(E)} - \sum_{l'} v_{ll'}^{(E)} + 12a_2^{(E)}\langle u_E^2 \rangle\right) \xi_0'(T)$$

$$+4a_2^{(E)}\xi_0'^3(T) = C'\xi_0(T)\,, \tag{4.8}$$

where we have written the local E-mode potential as

$$V_E(\xi_l'^2) = a_1^{(E)}\xi_l'^2 + a_2^{(E)}\xi_l'^4\,, \tag{4.9}$$

and $\langle u_E^2\rangle$ is written as an abbreviated form of $\langle (u_l^{(E)})^2\rangle$. If the coupling C' is small, the static E-mode displacement is also small and becomes linearly proportional to the polar-mode displacement $\xi_0(T)$.

It follows that by virtue of the A_1-E coupling the E-modes can contribute directly to spontaneous polarization. Although this amount is in all probability small, the fact that the lowest E modes are thermally excited at lower temperatures than the soft mode may make their contribution to the *temperature deviation* of polarization much more significant. In fact, if we neglect for the moment any soft-mode contribution to this temperature deviation [i.e., $\xi_0(T) = \xi_0(0)$], Eqs. (3.11), (3.13), (3.14) retain their form in the E-mode context, giving

$$[\xi_0'(0) - \xi_0'(T)]/\xi_0'(0) = 3[2\xi_0'^2(0)]^{-1} \times \langle [\hbar/\Omega_{\vec{q}}^E(T)]\, e^{-\hbar\Omega_{\vec{q}}^E(T)/kT}\rangle_{\vec{q}}\,, \tag{4.10}$$

where $\Omega_{\vec{q}}^E(T)$ is the (self-consistent) E-mode frequency at wave vector $\vec{q}$ and temperature T.

Although the amplitude of the resulting contribution to the temperature dependence of spontaneous polarization requires a knowledge of both coupling constant C' and the optic-mode strength of the relevant E mode, the temperature dependence of the contribution [at least to the extent that $\Omega_{\vec{q}}^E(T)$ is temperature independent] is well defined and is again of form (3.16) or (3.18), depending on E-mode dispersion, but where t is now $kT/\hbar\Omega_0^E$ or $kT/\hbar\Omega_{\min}^E$ and K is an unspecified constant.

V. ANALYSIS OF EXPERIMENTAL RESULTS–STRAIN EFFECTS

The first observation which can be made from an analysis of Figs. 1 and 2 is independent of any proposed microscopic mechanism and is simply that the two experimental techniques, direct charge integration (CI) and infrared detection (ID), are not measuring the same temperature dependence of P_s' at low temperatures. The effect is particularly pronounced for $LiNbO_3$, and we shall discuss this case first.

Although the relative accuracy (i.e., shape) of the ID measurements of p/C is considerably higher than the absolute scale, the latter can be estimated from the room-temperature values of p and C. In principle, therefore, a knowledge of the temperature dependence of thermal capacity enables us to calculate the explicit temperature dependence of P_s' from the ID measurements by direct numerical integration, after which a comparison can be made with the CI measurements of the same nominal quantity. We are in possession of measured specific-heat data for $LiNbO_3$ down to[9] 80 °K and again below 10 °K.[21] At very low temperatures a Debye law is found with Debye temperatures $\Theta_D = 560$ °K. We expect this law to hold only at temperatures small compared to the energy of the lowest optic mode, but it is not difficult to interpolate smoothly between this very-low-temperature behavior and the measurements for $T > 80$ °K given in Ref. 9 (see Fig. 4). An added difficulty arises from the fact that neither the ID nor CI measurements can be continued to arbitrarily low temperatures, so that some uncertainty remains as to the precise limiting value of $P_s'(T)$ and p/C as $T \to 0$. Although this uncertainty is minute in absolute terms, amounting to only a few parts in 10^7 of the limiting value itself, it obviously affects an estimate of polarization deviation $P_s'(0) - P_s'(T)$ seriously at low enough temperatures.

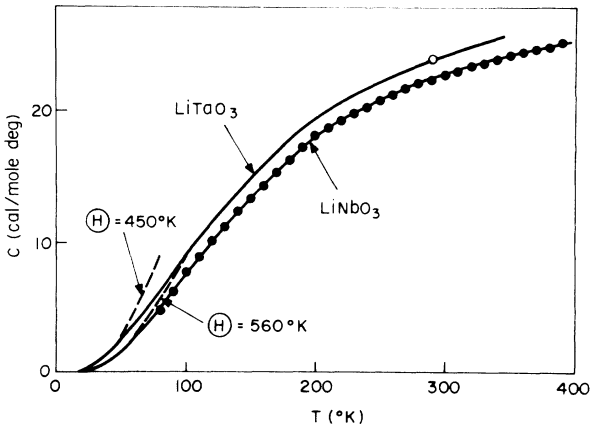

FIG. 4. Since specific heat for $LiNbO_3$ $LiTaO_3$ has to date not been measured continuously from very low temperatures to room temperature, some interpolation has been necessary in deducing the curves of specific heat C shown in this figure. Solid circles are measured data for $LiNbO_3$ from Ref. 9. Below 10 °K the niobate C follows a Debye law with Debye temperature $\Theta \approx 560$ °K (Ref. 21). This Debye law (shown dashed) is used to interpolate (full curve) between the $T < 10$ °K and $T > 80$ °K niobate data. For $LiTaO_3$ only the room-temperature C (open circle, Ref. 10) and low-temperature data (Ref. 22) below 10 °K have been published. The latter indicate a Debye law with $\Theta = 450$ °K. This curve (dashed) has been smoothly joined to the room-temperature measurement using the isomorphic niobate specific heat as a guide.

The direct comparison of $\Delta P_s' = P_s'(0) - P_s'(T)$ as a function of temperature (for $LiNbO_3$) as obtained from the two (ID and CI) methods is shown in Fig. 5. The curves are quite different. At high temperatures, ~300 °K, the percentage difference (~30%) is least and may be due to combined experimental errors. At very low temperatures (below

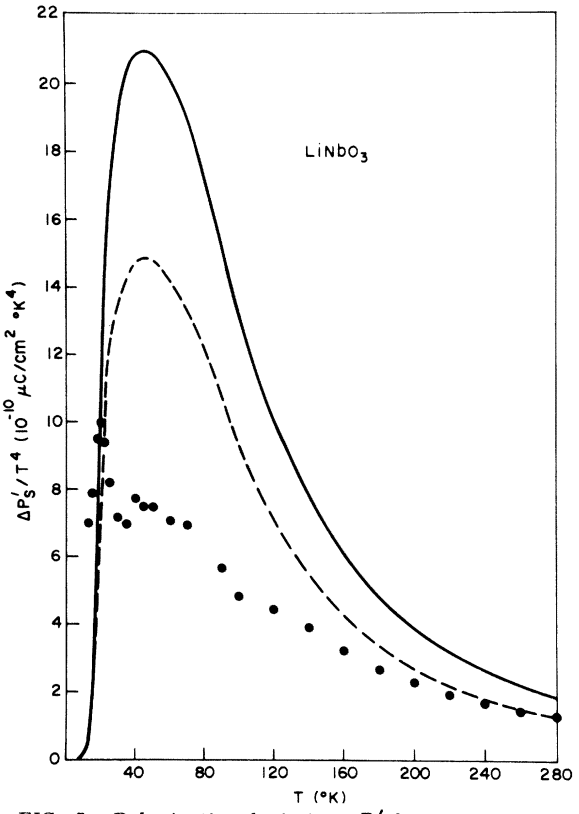

FIG. 5. Polarization deviation $\Delta P_s'$ from its value at absolute zero as measured for $LiNbO_3$ by the charge integration techniques of Sec. II A (closed circles) and as calculated from the pyroelectric data of Fig. 2(b) using the thermal-capacity interpolated curve of Fig. 4 (full curve). Also shown (dashed) is an equivalent pyroelectric curve scaled to fit the charge integration data at room temperature.

<30 °K) a lack of knowledge of the precise value of $P_s'(0)$ could play a role and give rise to the data scatter seen in Fig. 5. In the region of temperature above ~40 °K, however, the effect of the uncertainty in $P_s'(0)$ is negligible, so that in this region the comparison should be good to within the "scaling" accuracy (i.e., the combined errors in C and p at room temperature). In fact, from Fig. 5, we find a discrepancy at 40–60 °K of as much as a factor 3. A second method of "scaling," that of assuming that the two methods necessarily measure the same $\Delta P_s'(T)$ at room temperature, still leads qualitatively to a similar discrepancy at low temperatures (dashed curve in Fig. 5).

The equivalent comparisons for $LiTaO_3$ are instructive. Here we have experimental specific-heat data only below[22] 10 °K and at room temperature.[10] At low temperatures a Debye law is satisfied with $\Theta_D \approx 450$ °K and at room temperature $C \approx 24$ cal/mole °K. Using an interpolated C indicated and described in Fig. 4 we find this time a much smaller discrepancy between the ID and CI estimates for polarization deviation (Fig. 6). In fact, much if not all of the difference can probably be attributed to the lack of precise C data and the experimental accuracy. The CI values are some 30% less than the derived ID values throughout, and if "scaled" to agree at room temperature (dashed curve in Fig. 6) an essential agreement at all temperatures is produced. However it is pertinent to note that the rate of decrease of spontaneous polarization at low temperatures is very much larger in the tantalate than the niobate, and that the large relative discrepancy between CI and ID data in Fig. 5 for $LiNbO_3$ would, in absolute terms, go essentially unnoticed in the tantalate context.

We feel that the likely cause of the above discrepancy is an increasing effective clamping of the transverse (perpendicular to the c axis) dimensions in the ID experiments due to a decreasing thermal conductivity as the temperature decreases. Thus, at low temperatures, the heat pulse and resulting pyroelectric response may only probe the reaction of a layer whose transverse piezoelectric reaction is effectively clamped by the unperturbed bulk ferroelectric. If this is in fact the case, we should expect a difference between the separate CI and ID contributions at low temperatures of the form [see Eq. (4.4)] $2e_{31}\alpha_1 dT + 2P_s\alpha_1 dT$, where e_{31} (in normal piezoelectric notation) is $d_{3i}c_{i1}$, and we have made use of the symmetry restriction for crystals in class $3m$. Integrating, we find

$$\Delta P_s'(\mathrm{ID}) - \Delta P_s'(\mathrm{CI}) = \int_0^T (2e_{31} + 2P_s)\alpha_1 \, dT \,, \quad (5.1)$$

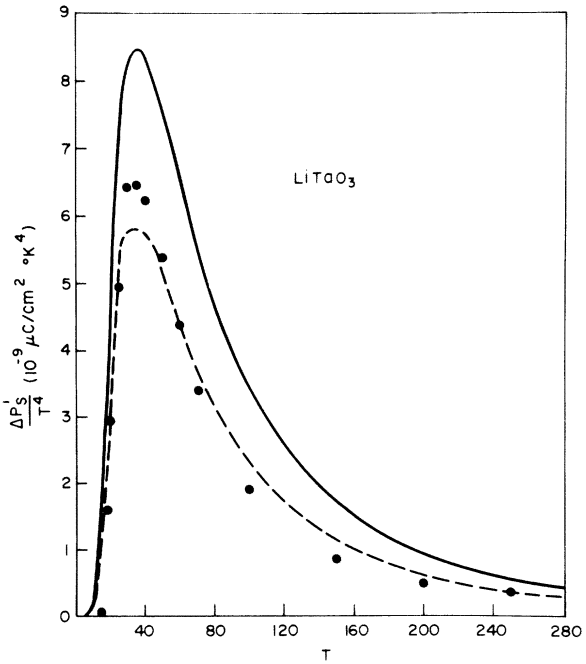

FIG. 6. As for Fig. 5 but for $LiTaO_3$.

where $\Delta P_s'(\mathrm{ID})$ and $\Delta P_s'(\mathrm{CI})$ are $P_s'(0) - P_s'(T)$ as measured, respectively, by dynamic pyroelectric and charge integration techniques.

Low-temperature spontaneous polarization is of order 70 $\mu C/cm^2$ in $LiNbO_3$ and 50 $\mu C/cm^2$ in $LiTaO_3$. Piezoelectric stress constant ϵ_{31} has been measured at and above room temperature only.[19] However, it shows only a slight temperature dependence near room temperature and is not expected to be anomalous as $T \to 0$. We therefore use the room-temperature values $e_{31} \approx +23$ $\mu C/cm^2$ ($LiNbO_3$) and $e_{31} \approx -38$ $\mu C/cm^2$ as crude low-temperature estimates. It is now evident from (5.1) that $\Delta P_s'(\mathrm{ID}) - \Delta P_s'(\mathrm{CI})$ is positive in $LiNbO_3$, in agreement with observations, but is absolutely smaller (and possibly even of uncertain sign) in the tantalate. To obtain a more detailed temperature dependence requires a knowledge of the low-temperature form of the thermal-expansion coefficient α_1. As a starting point we take the Grüneisen approximation

$$\alpha_i = \gamma_i c_v / K_T \,, \tag{5.2}$$

where c_v is the specific heat, K_T is the isothermal compressibility, and γ_i is the so-called Grüneisen parameter. For simple monoatomic lattices K_T and γ_i are usually fairly constant over a large temperature range, in which case $\alpha_i \propto c_v$. In lattice structures of the complexity of $LiNbO_3$ and $LiTaO_3$ this proportionality to specific heat is valid only at temperatures low enough for the Debye approximation to be realistic, i.e., temperatures for which the optic phonons are not appreciably populated. It follows that in this temperature range we can write $\alpha_i \propto c_v \propto T^3$ and, substituting in (5.1), it follows that

$$\Delta P_s'(\mathrm{ID}) - \Delta P_s'(\mathrm{CI}) = B(e_{31} + P)T^4 \,, \quad T \to 0 \tag{5.3}$$

where B is a positive constant.

The absolute value of B cannot be estimated from the known room-temperature thermal-expansion coefficients with more than order-of-magnitude accuracy, but an extension of the low-temperature form $\alpha_i \propto c_v$ to room temperature would suggest $B \sim (5\text{–}10) \times 10^{-12}\ ^\circ\mathrm{K}^{-4}$ in these materials and is indeed the right order of magnitude to account for the observed discrepancy between the pyroelectric and charge integration measurements of $\Delta P_s'$ in Fig. 5 for $LiNbO_3$. We should stress, however, that the T^4 relationship of (5.3) may well break down for $T \gtrsim 40\ ^\circ\mathrm{K}$, by which temperatures the contribution to α_i from a thermal population of the lowest optic mode is probably significant.

The important general point which emerges is that (excluding "Born" terms) for any but a completely clamped system the lowest-order temperature-dependent contribution to polarization deviation $P_s'(0) - P_s'(T)$ arises from pyroelectric and piezoelectric terms which go as the fourth power of absolute temperature,

$$\Delta P_s' = P_s'(0) - P_s'(T) \propto T^4 \,, \quad T \to 0 \,. \tag{5.4}$$

It is for this reason that we plot $\Delta P_s'/T^4$ as ordinate in Figs. 5 and 6. In general, it is not possible to predict the sign of the coefficient of proportionality in (5.3), although for $LiNbO_3$ and $LiTaO_3$, where the more specific relationship is

$$\Delta P_s' = -[B(e_{31} + P) + De_{33}]T^4 \,, \quad T \to 0 \tag{5.5}$$

with B and D positive (i.e., positive thermal-expansion coefficients), the room-temperature values of e_{31}, P, and e_{33}, which are[19] +23, +70, +133 $\mu C/cm^2$, respectively, for $LiNbO_3$ and −38, +50, +109 $\mu C/cm^2$, respectively, for $LiTaO_3$, indicate that $\Delta P_s'$ is initially *negative* in both cases. For (unprimed) real spontaneous polarization ΔP_s the only difference is that the P term in (5.5) is absent, i.e., $\Delta P_s = -(Be_{31} + De_{33})T^4$, which is again negative for $LiNbO_3$ but of uncertain sign in $LiTaO_3$.

If our interpretation of the polarization deviations as measured by CI and ID techniques is correct, then the charge integration method measures the full deviation of (5.5), i.e., $\Delta P_s'(\mathrm{CI}) = \Delta P_s'$, while the infrared detection method at very low temperatures measures

$$\Delta P_s'(\mathrm{ID}) = -De_{33}T^4 \,, \quad T \to 0 \,. \tag{5.6}$$

It follows that $p/C = (-1/C)dP_s'(\mathrm{ID})/dT$ should be negative at very low temperatures in both the tantalate and niobate. From Fig. 2(b) we see that there is indeed evidence for a change in sign of this quantity in one of the niobate samples as the temperature decreases below about 9 °K. However, at low temperatures the specific heat and thermal conductivity become so small that we suspect the heat pulse changes the crystal temperature by a significant fraction. The resulting response averaged over this temperature range obscures the limiting acoustic behavior predicted by (5.5). The low-temperature minima in p/C observed in about 7–8 °K in both materials [Figs. 2(a) and 2(b)] may be due to this effect, or to the decreasing thermal relaxation time of the crystal at very low temperature, or to the onset of a "Born" divergence.

In the niobate there is additional evidence in favor of negative values of $\Delta P_s'$ as $T \to 0$ in the charge integration measurements. The problem here is that an experimental measure of $\Delta P_s'(\mathrm{CI}) = \Delta P_s'$ requires a knowledge of the limiting value of spontaneous polarization $P_s'(0)$ at absolute zero. The zeros on the $\Delta P'$ ordinate axes of Figs. 1(a) and 1(b) were obtained by extrapolation from the lowest temperatures ($\approx 15\ ^\circ\mathrm{K}$) for which changes of $\Delta P'$ were measurable. This results in a large relative uncertainty in the absolute value of $\Delta P'(\mathrm{CI})$ below 20 °K. The very-low-temperature behavior of $\Delta P_s'/T^4$ in $LiNbO_3$ is quite irregular and different from

the equivalent tantalate results. If our explanation of the difference $\Delta P_s'(\mathrm{ID}) - \Delta P_s'(\mathrm{CI})$ is valid, then its sign in $LiNbO_3$ should certainly not change at very low temperatures in the manner suggested by the data in Fig. 5. Choosing a limiting $P_s'(0)$ to satisfy this requirement necessitates a negative slope for $\Delta P_s'(\mathrm{CI})$ as a function of T at very low temperatures with a turnover $\Delta P_s'(\mathrm{CI})/dT = 0$ at 10–12 °K, and with a change $\Delta P'$ between absolute zero and the maximum at ~10 °K of 10^{-4} $\mu C/cm^2$. There is no experimental evidence for the analogous effect in $LiTaO_3$.

VI. ANALYSIS OF EXPERIMENTAL RESULTS–DYNAMIC EFFECTS

Having obtained at least a qualitative understanding of the low-temperature acoustic-mode contributions to polarization we now turn to slightly higher temperatures and to the lowest optic-mode contributions. The ID measurements of Figs. 2(a) and 2(b) strictly contain acoustic- and optic-mode contributions, but the indications from Sec. V are that the former are very small in a relative sense in $LiTaO_3$. We can therefore attempt to understand Fig. 2(a) solely in terms of optic-mode effects. The situation for $LiNbO_3$ is less clear, and the acoustic contributions to the ID curve of Fig. 2(b) may be relatively more important. Very obviously, however, the curves of Figs. 2(a) and 2(b) are qualitatively the same, particularly as regards the fast increase of p/C up to a maximum at ~30 K. We shall therefore suppose that any acoustic-mode contribution to p/C in $LiNbO_3$ is a weakly temperature-dependent function at lower temperatures (it actually becomes a constant, corresponding to a simple shift of base line, at temperatures within the Debye region where we expect the Grüneisen

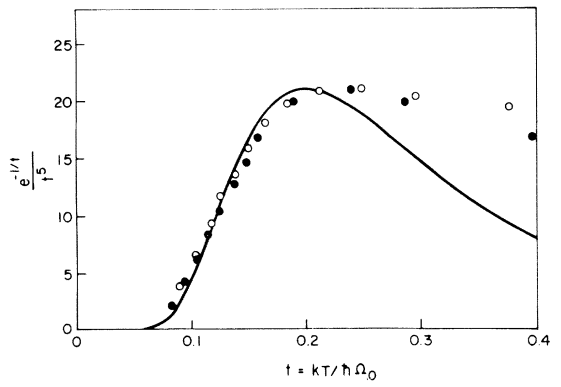

FIG. 7. Comparison of the low-temperature pyroelectric response data for $LiTaO_3$ [from Fig. 2(a)] and stoichiometric $^7LiNbO_3$ [from Fig. 2 (b)] with the theoretical form $t^{-5}e^{-1/t}$ of (6.1) corresponding to a flat mode dispersion. Open circles are for $LiTaO_3$ and correspond to an energy gap $\hbar\Omega_0 = 85$ cm^{-1}, while filled circles are for $LiNbO_3$ with an energy gap $\hbar\Omega_0 = 88$ cm^{-1}.

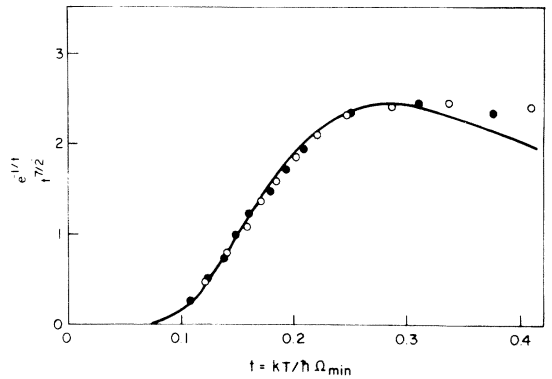

FIG. 8. As for Fig. 7 but using the theoretical form $t^{-7/2}e^{-1/t}$ of (6.2) for a quadratic energy minimum at $\hbar\Omega_{min}$ in optic-mode dispersion. Open circles are for $LiTaO_3$ and correspond to an energy gap $\hbar\Omega_{min} = 63$ cm^{-1}, while filled circles are for $LiNbO_3$ with an energy gap $\hbar\Omega_{min} = 67$ cm^{-1}.

relation to hold), so that the broad features of Fig. 2(b) can also be discussed in terms of optic-mode features alone.

For temperatures up to ~30 °K we expect the specific heat to follow a simple T^3 Debye law. We therefore anticipate from Secs. III and IV B that the lowest-temperature optic-mode contribution to ID response should vary as $T^{-3}d\epsilon/dT$, where $d\epsilon/dT$ is given by (3.16) for a flat mode response and by (3.18) for a well-developed quadratic minimum-band-energy response. We therefore compare the $LiTaO_3$ and $LiNbO_3$ ID response measurements with these two possible formalisms: first,

$$p/C = Kt^{-5}e^{-1/t}, \quad t = kT/\hbar\Omega_0, \tag{6.1}$$

in Fig. 7, and second,

$$p/C = K't^{-7/2}e^{-1/t}, \quad t = kT/\hbar\Omega_{min}, \tag{6.2}$$

in Fig. 8. A qualitative fit to (6.1) can be obtained up to the maximum in the response at $T \approx 30$ °K if the flat mode energy is $\hbar\Omega_0 = 85$ cm^{-1} in $LiTaO_3$ and $\hbar\Omega_0 = 88$ cm^{-1} in $LiNbO_3$. These energies are way below that of the zone-center soft mode and even below the lowest well-documented long-wavelength E mode (≈ 140 cm^{-1}). They are however close to the energies of the disputed E modes claimed by Kaminow and Johnston[12] to be responsible for an observed Raman response in this energy range (≈ 70 cm^{-1} in $LiTaO_3$ and ≈ 90 cm^{-1} in $LiNbO_3$). Speculation, however, is not warranted since a significantly better fit to the data is obtained by use of (6.2); see Fig. 8. Here the fit is quantitative up to the maximum of the response ($T \approx 30$ °K) if the band minimum responsible is at $\hbar\Omega_{min} \approx 63$ cm^{-1} in $LiTaO_3$ and 67 cm^{-1} in $LiNbO_3$. These energies need not correspond to any long-wavelength optic mode since they could occur any-

where in the Brillouin zone. The agreement between the theory of (6.2) and experiment breaks down rapidly above 30 °K and the reasons are many. First, the specific-heat T^3 law breaks down above ~30 °K. Second, the quadratic dispersion law giving rise to (6.2) will probably cease to be an adequate representation of the band energy at temperatures much higher than 30 °K. Third, if the mode responsible for the low-temperature response is not the soft mode, we must expect the A_1 soft-mode contribution to become significant and eventually to dominate at higher temperatures.

In the absence of inelastic neutron measurements of the complete lattice mode dispersion curves it is really not possible to determine whether the 60–70-cm^{-1} excitation energies responsible for the 30 °K maximum in ID response result from the A_1 soft mode or not. The possibility of a dynamic E-mode mechanism certainly cannot be dismissed at this stage, although the possibility of a static E-mode coupling to polarization via strain has been ruled out by the high-frequency (i.e., clamped) observations of Fig. 2(a) on $LiTaO_3$. In fact, the sensitivity of the quantitative ID response to crystal sample possibly lends support to an E-mode picture, but is far from conclusive.

VII. CONCLUSIONS

We have used charge integration and dynamic pyroelectric techniques to measure the temperature dependence of low-temperature spontaneous polarization in $LiNbO_3$ and $LiTaO_3$. These techniques do not, in fact, measure spontaneous electric moment per unit volume P_s but a closely related quantity P_s' whose temperature derivative is simply related to that of spontaneous polarization dP_s/dT by

$$\frac{dP_s'}{dT} = \frac{dP_s}{dT} + 2\alpha_1 P_s , \tag{7.1}$$

where α_1 is the linear thermal-expansion coefficient perpendicular to the polar direction. We find, in particular, that a derived low-temperature theoretical form

$$\frac{dP_s'}{dT} = K_1' T^3 + K_2' T^{-1/2} e^{-\hbar\Omega/kT} + \cdots \tag{7.2}$$

is quantitatively able to account for the experimental findings up to about 30–40 °K in general. In (7.2) the first term arises from the thermal population of acoustic modes via volume expansion and piezoelectric strain, while the second results from the thermal population of a low-energy optic lattice mode with a band minimum energy gap $\hbar\Omega$ not necessarily occurring at a Brillouin-zone center.

Since the linear expansion coefficient is, from the Grüneisen approximation, expected to vary as T^3, at low temperatures we expect the algebraic form (7.2) to be valid also for spontaneous polarization proper, i.e.,

$$\frac{dP_s}{dT} = K_1 T^3 + K_2 T^{-1/2} e^{-\hbar\Omega/kT} , \tag{7.3}$$

where $K_2 \approx K_2'$. The constant $K_2 \approx K_2'$ is found to be negative in both $LiNbO_3$ and $LiTaO_3$ and produces a decrease of spontaneous polarization with increasing temperature. However, at very low temperatures, the acoustic T^3 term is found to dominate and although K_1 is of uncertain sign in $LiTaO_3$, it is definitely positive (as is K_1') in $LiNbO_3$. It follows that for the niobate the spontaneous polarization at the very lowest temperatures first increases with increasing temperature. This increase is small, amounting in relative terms to no more than one part in 10^6 of the total polarization, with the latter going through a maximum at $T \sim 10$ °K before beginning its fall eventually to zero at the Curie point.

High-frequency measurements performed on an effectively clamped $LiTaO_3$ sample establish that the exponential terms in (7.2) or (7.3) are of direct dynamic origin, i.e., do not depend upon a coupling to strain. The fit of theory with experiment produces estimates $\hbar\Omega \approx 60$–70 cm^{-1} for optic-mode energy gap in both materials. Since no zone-center optic mode is thought to have this low an energy we must suppose that this band minimum occurs away from the zone center. It is not possible to tell whether the phonon band which contains this mode is that which eventually softens at the Curie point or not.

It is evident from both the experimental data and the theory that the performance of $LiTaO_3$ and $LiNbO_3$ as infrared detectors may be improved at temperatures near 30 °K, where the responsivity is greater than at room temperature and thermal noise is decreased. At lower temperatures no improvement is expected since secondary contributions to the pyroelectric response are considerably smaller than the primary contributions from anharmonic optic modes. Indeed, in general terms, we can conclude for materials in which the dominant contributions to the pyroelectric response come from an optic mode of low frequency Ω, the maximum responsivity occurs at temperatures in the neighborhood of $kT \sim (0.2$–$0.3)\hbar\Omega$, unless, at extremely low temperatures indeed, the Born divergence materializes.

ACKNOWLEDGMENT

It is a pleasure to thank T. J. Negran for his expert technical assistance.

[1]W. Ackermann, Ann. Phys. (Leipz.) 46, 197 (1915).
[2]M. Born, Rev. Mod. Phys. 17, 245 (1945).
[3]G. Heiland and H. Ibach, Solid State Commun. 4, 353 (1966).
[4]C. G. B. Garrett, IEEE J. Quantum Electron. QE-4, 70 (1968).
[5]V. V. Gladkii and I. S. Zheludev, Kristallografiya 10, 50 (1965) [Sov. Phys.-Crystallogr. 10, 63 (1965)].
[6]S. B. Lang, Phys. Rev. B 4, 3603 (1971).
[7]A. M. Glass, J. Appl. Phys. 40, 4699 (1969).
[8]A. G. Chynoweth, J. Appl. Phys. 27, 78 (1956).
[9]V. V. Zhdanova, V. P. Klyuev, V. V. Lemanov, I. A. Smirnov, and V. V. Tikhonov, Fiz. Tverd. Tela 10, 1725 (1968) [Sov. Phys.-Solid State 10, 1360 (1968)].
[10]A. M. Glass, Phys. Rev. 172, 564 (1968).
[11]A. S. Barker and R. Loudon, Phys. Rev. 158, 433 (1967).
[12]W. D. Johnston and I. P. Kaminow, Phys. Rev. 168, 1045 (1968).
[13]M. E. Lines, Phys. Rev. B 9, 950 (1974).
[14]M. R. Chowdhury, G. E. Peckham, R. T. Ross, and D. H. Saunderson, J. Phys. C 7, L99 (1974).
[15]R. Claus, G. Borstel, E. Wiesendanger, and L. Steffan, Z. Naturforsch. A 27, 1187 (1972).
[16]A. S. Barker, A. A. Ballman, and J. A. Ditzenberger, Phys. Rev. B 2, 4322 (1970).
[17]S. Devine and G. Peckham, J. Phys. C 4, 1091 (1971).
[18]W. G. Cady, *Piezoelectricity* (Dover, New York, 1964).
[19]R. T. Smith and F. S. Welsh, J. Appl. Phys. 42, 2219 (1971).
[20]Y. Yamada, H. Iwasaki, and N. Niizeki, Jap. J. Appl. Phys. 8, 1127 (1969).
[21]J. Bergman (private communication).
[22]J. Warta (private communication), reported in Ref. 8.

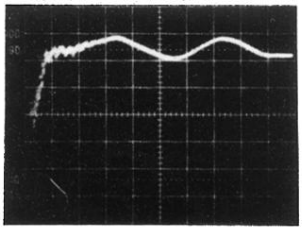

FIG. 3. Oscilloscope trace showing the initial clamped pyroelectric response $\Delta P'$ followed by slowly varying oscillations due to secondary pyroelectricity upon thermal expansion of the crystal.